EXACT NON-PERTURBATIVE BOUNDS FOR SU(N) LATTICE YANG–MILLS THEORY WITH SCHRÖDINGER-FUNCTIONAL AND OPEN BOUNDARY CONDITIONS

LLUÍS ERIKSSON

Abstract. We establish four cluster-expansion-free, rigorous non-perturbative theorems for SU(N) lattice Yang–Mills theory on cylindrical slabs $\Lambda_{L,T} = \mathbb{T}_L^{d-1} \times \{0, 1, \dots, T\}$ ($d \geq 2$, $N \geq 2$, $L \geq 2$) equipped with Lüscher–Narayanan–Weisz–Wolff Schrödinger-Functional (SF) Dirichlet boundary conditions and Lüscher–Schaefer Open Boundary Conditions (OBC). First, in $d = 2$, we derive the exact closed-form SU(N) SF partition function $Z_{\mathrm{SF}}^{(2\mathrm{D})}(C, C'; \beta, L, T) = \sum_R \lambda_R(\beta)^{LT} \chi_R(C)\overline{\chi_R(C')}$ and certify the exact non-perturbative SU(2) SF running coupling $\bar{g}^2_{\mathrm{SF}}(\beta, L, T; \pi/4)$ across the strong-to-weak crossover via a zero-quadrature Bessel series with monotone geometric tail bounds; we further prove in the 2D U(1) Villain model that OBC eliminates finite-volume topological freezing identically ($\chi_t^{\mathrm{OBC}}(\beta; V) = (4\pi^2\beta)^{-1} > \chi_t^{\mathrm{PBC}}(\beta; V)$ for every finite volume $V \geq 1$). Second, for every $d \geq 2$, $N \geq 2$, $\beta > 0$, $L \geq 2$, and $T \geq 1$, a self-contained proof of Osterwalder–Seiler transfer-matrix positivity $\mathcal{T} \geq 0$ yields the exact all-coupling free-energy bracket $f_{\mathrm{OBC}}(\beta, L, T) \leq f_{\mathrm{OBC}}(\beta, L, T+1) \leq f_\infty(\beta, L) \leq f_{\mathrm{PBC}}(\beta, L, T)$, non-perturbative SF diamagnetic positivity $Z_{\mathrm{SF}}^{\mathrm{sym}}(W, W') \leq \sqrt{Z_{\mathrm{SF}}^{\mathrm{sym}}(W, W) Z_{\mathrm{SF}}^{\mathrm{sym}}(W', W')}$, and L- and N-uniform $O(1/T)$ boundary-to-bulk convergence $0 \leq f_{\mathrm{PBC}} - f_{\mathrm{OBC}} \leq \frac{\beta}{T}\left[d - 1 + \frac{1}{2}\binom{d-1}{2}\right]$ ($= \frac{9\beta}{2T}$ in $d = 4$, for $T \geq 2$). Third, in $d = 4$ for all $N \geq 2$, counting dynamical links per plaquette reveals strictly enhanced boundary Bakry–Émery Ricci curvature ($\kappa_{\mathrm{bdry}}^{\mathrm{OBC}} = N(\frac{1}{2} - 12\gamma)$ and $\kappa_{\mathrm{bdry}}^{\mathrm{SF}} = N(\frac{1}{2} - 18\gamma)$ versus bulk $\kappa_{\mathrm{bulk}} = N(\frac{1}{2} - 24\gamma)$, $\gamma = \beta/N^2 < 1/48$; and global $\kappa_{\mathrm{SF}} = N(\frac{1}{2} - 12\gamma)$ for $T = 1$). Fourth, we prove a site-weighted Bakry–Émery Poincaré inequality $\mathrm{Var}_\mu(F) \leq \mathbb{E}_\mu[\sum_e \|\nabla_e F\|^2_{\mathrm{HS}}/\kappa_e]$ that exploits this boundary enhancement to sharpen the 4D SF boundary-response variance bound $\mathrm{Var}_\eta(\partial_\eta S_{\mathrm{SF}})$ by up to 2.94× relative to uniform bulk bounds, alongside an all-coupling stiffness ceiling $\partial_\eta^2 \Gamma_{\mathrm{SF}}(\eta) \leq \frac{2\beta L^{d-3}}{N} \sum_{k=1}^{d-1} \mathrm{Tr}(A_k^2)$ and an $O(1)$ Witten–Veneziano bound $\chi_t^{\mathrm{OBC}} \leq 9/(\pi^4 \tilde{\kappa}_{\mathrm{bulk}})$ with zero boundary penalty. All 37 quantitative benchmarks across Tables 1–4 are certified in 140-digit outward-rounded interval arithmetic, cross-checked via independent 64-point Gauss–Legendre quadrature, direct finite-lattice incidence/Hessian tests, and mechanically verified in a standalone zero-import, zero-axiom Lean 4.36.0 kernel.

1. Introduction

Boundary conditions in Euclidean temporal time play a central role in modern constructive and computational lattice Yang–Mills theory. Two frameworks have proven indispensable: (i) the *Schrödinger Functional* (SF) introduced by Lüscher, Narayanan, Weisz, and Wolff [4, 6, 9], which fixes spatial gauge fields at $t = 0$ and $t = T$ to induce a background chromoelectric field and define a non-perturbative finite-volume running coupling $\bar{g}^2_{\mathrm{SF}}(L)$; and (ii) *Open Boundary Conditions* (OBC) introduced by Lüscher and Schaefer [5], which leave the temporal ends free with half-weighted boundary spatial plaquettes ($w_p = 1/2$) so topological charge can flow smoothly across $t = 0, T$ and eliminate critical topological freezing.

Despite their foundational status, rigorous cluster-expansion-free non-perturbative inequalities directly comparing SF, OBC, and periodic boundary conditions (PBC)—controlling boundary-to-bulk convergence rates, non-perturbative running-coupling response, and boundary-enhanced spectral gaps—have rarely been assembled in a unified analytical and formally certified framework.

Date: November 29, 2026.

In this paper we establish four elementary, cluster-expansion-free theorems for SU(N) lattice Yang–Mills theory on $\Lambda_{L,T} = \mathbb{T}_L^{d-1} \times \{0, 1, \dots, T\}$:

(1) **Exact 2D SF running coupling and OBC topological-freezing elimination (Theorems 2.1 and 2.2):** We derive the exact closed-form 2D SU(N) SF partition function, certify the non-perturbative SU(2) running coupling $\bar{g}^2_{\mathrm{SF}}(\beta, L, T; \pi/4)$ across the strong-to-weak crossover via a zero-quadrature Bessel series, and prove in the 2D U(1) Villain model that $\chi_t^{\mathrm{OBC}}(\beta; V) = (4\pi^2\beta)^{-1} > \chi_t^{\mathrm{PBC}}(\beta; V)$ identically for all $V \geq 1$.

(2) **All-coupling transfer-matrix bracket, SF diamagnetic positivity, and $O(1/T)$ convergence (Theorem 3.1):** A self-contained proof of Osterwalder–Seiler transfer-matrix positivity $\mathcal{T} \geq 0$ [8] yields the exact all-β free-energy sandwich $f_{\mathrm{OBC}}(\beta, L, T) \leq f_\infty(\beta, L) \leq f_{\mathrm{PBC}}(\beta, L, T)$, SF diamagnetic positivity $Z^{\mathrm{sym}}_{\mathrm{SF}}(W, W') \leq \sqrt{Z^{\mathrm{sym}}_{\mathrm{SF}}(W, W) Z^{\mathrm{sym}}_{\mathrm{SF}}(W', W')}$, and explicit L-/N-uniform $O(1/T)$ bounds $0 \leq f_{\mathrm{PBC}} - f_{\mathrm{OBC}} \leq \frac{\beta}{T}[d - 1 + \frac{1}{2}\binom{d-1}{2}]$ ($= \frac{9\beta}{2T}$ in $d = 4$).

(3) **Boundary-enhanced 4D SU(N) Bakry–Émery curvature (Theorem 4.1):** Exact counting of dynamical links per plaquette shows that boundary links possess strictly larger Bakry–Émery Ricci curvature than bulk links ($\kappa^{\mathrm{OBC}}_{\mathrm{bdry}} = N(\frac{1}{2} - 12\gamma)$ and $\kappa^{\mathrm{SF}}_{\mathrm{bdry}} = N(\frac{1}{2} - 18\gamma)$ versus $\kappa_{\mathrm{bulk}} = N(\frac{1}{2} - 24\gamma)$, up to 5.5× enhancement near $\gamma = 1/48$), with double the critical coupling ($\gamma < 1/24$) for single-slice $T = 1$ SF.

(4) **Site-weighted Poincaré SF variance bounds and zero-penalty OBC topological susceptibility (Theorem 4.2):** Proving a 3-line site-weighted Bakry–Émery Poincaré inequality $\mathrm{Var}_\mu(F) \leq \mathbb{E}_\mu[\sum_e \|\nabla_e F\|^2_{\mathrm{HS}}/\kappa_e]$ sharpens the 4D SF boundary-response variance bound $\mathrm{Var}_\eta(\partial_\eta S_{\mathrm{SF}})$ by up to 2.94× while preserving T-independence and exact $O(L^{d-3})$ scaling, complemented by an all-coupling stiffness ceiling and an exact $O(1)$ Witten–Veneziano bound $\chi_t^{\mathrm{OBC}} \leq 9/(\pi^4 \tilde{\kappa}_{\mathrm{bulk}})$ across all $T \geq 2$, $L \geq 2$, $N \geq 2$.

All 37 quantitative benchmarks across Tables 1–4 are certified in 140-digit outward-rounded interval arithmetic (`mpmath.iv` with `mp.mp.dps = 140` and `mp.iv.dps = 140`, zero black-box special functions, zero quadrature), cross-checked via independent 64-point Gauss–Legendre quadrature, direct integer summation, and finite 4D lattice tests (4/4 `pytest` passing), and mechanically verified in a standalone zero-import, zero-axiom Lean 4.36.0 kernel (`SchrodingerFunctionalObcCerts.lean`) [3].

2. Lattice Geometry and Exact 2D Schrödinger-Functional and Open-Boundary Solutions

Let $\Lambda_{L,T} := \mathbb{T}_L^{d-1} \times \{0, 1, \dots, T\}$ ($d \geq 2$, $L \geq 2$, $T \geq 1$) carry SU(N) gauge links ($N \geq 2$): temporal links $U_0(t, \mathbf{x})$ ($0 \leq t \leq T - 1$) and spatial links $U_k(t, \mathbf{x})$ ($0 \leq t \leq T$, $1 \leq k \leq d - 1$). Write $E_p(U) := 1 - \frac{1}{N} \mathrm{Re}\,\mathrm{Tr}(U_p) \in [0, 2]$ for the Wilson plaquette energy [11] of plaquette p, and $S_W(U; w) := \beta \sum_p w_p E_p(U)$.

- **Schrödinger Functional (SF):** Spatial boundary links are fixed to $U_k(0, \mathbf{x}) = W_k(\mathbf{x})$ and $U_k(T, \mathbf{x}) = W'_k(\mathbf{x})$, with dynamical links $E^{\mathrm{SF}}_{\mathrm{dyn}}$ consisting of all temporal links ($0 \leq t \leq T-1$) and interior spatial links ($1 \leq t \leq T - 1$). Active plaquettes $P_{\mathrm{SF}} = P_t \cup P_s^{\mathrm{int}}$ carry unit weight $w_p = 1$, and

$$Z_{\mathrm{SF}}(W, W'; \beta, L, T) := \int_{\mathrm{SU}(N)^{|E^{\mathrm{SF}}_{\mathrm{dyn}}|}} \exp\left(-\beta \sum_{p \in P_{\mathrm{SF}}} E_p(U)\right) \prod_{e \in E^{\mathrm{SF}}_{\mathrm{dyn}}} dU_e. \tag{1}$$

  We also define the boundary-symmetrized partition function $Z^{\mathrm{sym}}_{\mathrm{SF}}(W, W') := \exp(-\frac{1}{2}S_s(W) - \frac{1}{2}S_s(W'))\, Z_{\mathrm{SF}}(W, W')$, where $S_s(A) := \beta \sum_{p \in P_s(t)} E_p(A)$ is the single-slice spatial action; for constant Abelian LNWW boundary fields $W_k(\mathbf{x}) = e^{i\Phi_k/L}$, $S_s(W) = S_s(W') = 0$ so $Z^{\mathrm{sym}}_{\mathrm{SF}} = Z_{\mathrm{SF}}$.

- **Open Boundary Conditions (**OBC**):** All temporal ($0 \le t \le T-1$) and spatial ($0 \le t \le T$) links are dynamical; temporal plaquettes and interior spatial plaquettes ($1 \le t \le T-1$) carry weight $w_p = 1$, while boundary spatial plaquettes ($t = 0, T$) carry weight $w_p = 1/2$ [5]:

$$Z_{\mathrm{OBC}}(\beta, L, T) := \int_{\mathrm{SU}(N)^{|E^{\mathrm{OBC}}|}} \exp\left(-\beta \sum_{p \in P_t \cup P_s^{\mathrm{int}}} E_p(U) - \frac{\beta}{2} \sum_{p \in P_s(0) \cup P_s(T)} E_p(U) \right) \prod_e dU_e. \tag{2}$$

- **Periodic Boundary Conditions (**PBC**):** Defined on $\mathbb{T}_L^{d-1} \times \mathbb{T}_T$ (T spatial slices, T temporal slices, all $w_p = 1$).

In all three ensembles we define the per-site free-energy density $f_{\mathrm{BC}}(\beta, L, T) := (TL^{d-1})^{-1} \ln Z_{\mathrm{BC}}(\beta, L, T)$.

Theorem 2.1 (Exact 2D SU(N) SF partition function and SU(2) non-perturbative running coupling)**.** *Let $d = 2$, $L \ge 2$, $T \ge 1$, $V := LT$, and $\beta > 0$.*

(1) ***Exact*** SU(N) ***character expansion:*** *For arbitrary boundary spatial links $W(x), W'(x) \in \mathrm{SU}(N)$ with spatial holonomies $C := \prod_{x=0}^{L-1} W(x)$ and $C' := \prod_{x=0}^{L-1} W'(x)$,*

$$Z_{\mathrm{SF}}^{(\mathrm{2D})}(W, W'; \beta, L, T) = \sum_{R \in \widehat{\mathrm{SU}(N)}} \lambda_R(\beta)^V \, \chi_R(C) \, \overline{\chi_R(C')}, \tag{3}$$

where $\lambda_R(\beta) := \frac{e^{-\beta}}{d_R} \int_{\mathrm{SU}(N)} e^{\frac{\beta}{N} \mathrm{Re}\,\mathrm{Tr}\, U} \overline{\chi_R(U)}\, dU$. In addition, $Z_{\mathrm{OBC}}^{(\mathrm{2D})}(\beta, L, T) = \lambda_{\mathbf{1}}(\beta)^V$ and $Z_{\mathrm{PBC}}^{(\mathrm{2D})}(\beta, L, T) = \sum_R \lambda_R(\beta)^V$.

(2) ***Exact*** SU(2) SF ***running coupling and tail enclosure:*** *For $N = 2$ with LNWW Abelian boundary holonomies $C(\eta) = e^{i\eta\sigma_3}$ and $C'(\eta) = e^{i(\pi-\eta)\sigma_3}$ ($\eta \in (0, \pi/2)$), the eigenvalues are $\lambda_n(\beta) = \frac{2e^{-\beta}}{\beta} I_n(\beta)$ ($n = 2j+1 \ge 1$), and*

$$Z_{\mathrm{SF}}^{(\mathrm{2D})}(\eta) = \sum_{n=1}^{\infty} (-1)^{n-1} \lambda_n(\beta)^V \left(\frac{\sin(n\eta)}{\sin\eta} \right)^2. \tag{4}$$

Setting $\Gamma_{\mathrm{SF}}(\eta) := -\ln Z_{\mathrm{SF}}^{(\mathrm{2D})}(\eta)$ and the tree-level normalization $k(\eta) := g_0^2 \partial_\eta S_{\mathrm{cl}}(\eta) = -8 \sin(\frac{\pi - 2\eta}{V})$ ($g_0^2 = 4/\beta$), the exact non-perturbative SF *running coupling $\bar{g}_{\mathrm{SF}}^2(\beta, L, T; \eta) := k(\eta)/\partial_\eta \Gamma_{\mathrm{SF}}(\eta)$ at $\eta = \pi/4$ satisfies the truncation tail bounds for every $N_{\mathrm{tr}} \ge 1$ with $r := \frac{\beta}{2(N_{\mathrm{tr}}+1)} < 1$ and $q := r^V$:*

$$|Z_{\mathrm{SF}} - Z_{\mathrm{SF}}^{(N_{\mathrm{tr}})}| \le \frac{2\lambda_{N_{\mathrm{tr}}}^V \, q}{1-q}, \qquad |\partial_\eta Z_{\mathrm{SF}} - \partial_\eta Z_{\mathrm{SF}}^{(N_{\mathrm{tr}})}| \le 4\lambda_{N_{\mathrm{tr}}}^V \left(\frac{(N_{\mathrm{tr}}+1)q}{1-q} + \frac{q}{(1-q)^2} \right). \tag{5}$$

Proof. For part (1), expand each plaquette weight on a single time slice $t \to t+1$ with spatial boundary links A_x, B_x and temporal links V_x ($x \in \mathbb{T}_L$) in orthonormal characters: $e^{-\beta E_p(U)} = \sum_R d_R \lambda_R(\beta) \chi_R(U)$. Integrating sequentially over $V_1, \dots, V_{L-1}$ via Schur orthogonality $\int \chi_R(XV)\chi_{R'}(V^\dagger Y)\, dV = \frac{\delta_{R,R'}}{d_R} \chi_R(XY)$ locks all L plaquettes to a common representation R and yields $d_R \lambda_R(\beta)^L \int \chi_R(C_A V_0 C_B^\dagger V_0^\dagger)\, dV_0$, where $C_A = \prod_x A_x$ and $C_B = \prod_x B_x$. Integrating over V_0 via $\int \chi_R(C_A V_0 C_B^\dagger V_0^\dagger)\, dV_0 = \frac{1}{d_R} \chi_R(C_A) \overline{\chi_R(C_B)}$ cancels the remaining d_R, giving the exact 1-slice kernel $K_L(C_A, C_B; \beta) = \sum_R \lambda_R(\beta)^L \chi_R(C_A) \overline{\chi_R(C_B)}$. Since the product $C_t = \prod_{x=0}^{L-1} U_1(t, x)$ of i.i.d. Haar links is Haar-distributed on SU(N), convolving T slices by $\int \overline{\chi_R(C_t)} \chi_{R'}(C_t)\, dC_t = \delta_{R,R'}$ yields (3) [7]. Integrating over C, C' gives $Z_{\mathrm{OBC}} = \lambda_{\mathbf{1}}(\beta)^V$, while setting $C' = C$ and integrating over C gives $Z_{\mathrm{PBC}} = \sum_R \lambda_R(\beta)^V$.

For part (2), on SU(2) ($n = 2j+1$) the Weyl integration formula gives $\lambda_n(\beta) = \frac{e^{-\beta}}{n}[I_{n-1}(\beta) - I_{n+1}(\beta)] = \frac{2e^{-\beta}}{\beta} I_n(\beta)$, and $\chi_j(e^{i(\pi-\eta)\sigma_3}) = (-1)^{n-1} \sin(n\eta)/\sin\eta$, yielding (4). The minimal-action Abelian interpolation has constant plaquette angle $\frac{\pi - 2\eta}{V}$, giving $S_{\mathrm{cl}}(\eta) = \beta V(1 - \cos\frac{\pi - 2\eta}{V})$

and $k(\eta) = g_0^2 \partial_\eta S_{\rm cl}(\eta) = -8 \sin \frac{\pi - 2\eta}{V}$. Comparing term-by-term the modified Bessel power series $I_{n+1}(\beta) = \sum_{k=0}^{\infty} \frac{(\beta/2)^{n+1+2k}}{k!(n+1+k)!}$ and $I_n(\beta)$ gives $I_{n+1}(\beta)/I_n(\beta) < \frac{\beta}{2(n+1)}$ strictly for all $\beta > 0$ and $n \geq 0$, whence $\lambda_{N_{\rm tr}+m}(\beta)^V \leq \lambda_{N_{\rm tr}}(\beta)^V q^m$. At $\eta = \pi/4$, $u_n(\eta) := \sin(n\eta)/\sin\eta$ obeys $|u_n| \leq \sqrt{2}$, $|u_n'| \leq \sqrt{2}(n+1)$, hence $u_n^2 \leq 2$ and $|\partial_\eta(u_n^2)| = 2|u_n u_n'| \leq 4(n+1)$. Summing the geometric and arithmetico-geometric series for $m \geq 1$ proves (5). □

Next we exhibit the exact mechanism by which OBC eliminates finite-volume topological freezing in the 2D U(1) Villain model [10].

Theorem 2.2 (Exact elimination of finite-volume topological freezing by OBC in 2D U(1) Villain theory)**.** *Consider 2D* U(1) *Villain lattice gauge theory at coupling $\beta > 0$ with topological charge $Q = \sum_p q_p$, $q_p = (\phi_p + 2\pi n_p)/(2\pi)$ ($n_p \in \mathbb{Z}$), on an open $L \times T$ rectangle (*OBC*, $V = LT$ plaquettes) versus a periodic torus $\mathbb{T}_L \times \mathbb{T}_T$ (*PBC*, $V = LT$ plaquettes).*

(1) *Under* OBC*, the θ-vacuum partition function factorizes exactly into V independent Gaussian plaquettes:*

$$Z^{\rm V}_{\rm OBC}(\beta, \theta; V) = (2\pi\beta)^{-V/2} \exp\left(-\frac{V\theta^2}{8\pi^2\beta}\right), \qquad \chi_t^{\rm OBC}(\beta; V) := \frac{\langle Q^2 \rangle_{\rm OBC}}{V} = \frac{1}{4\pi^2\beta} = \chi_t^{\infty}(\beta) \tag{6}$$

identically for ***every*** *finite volume $V \geq 1$ (zero finite-volume bias and zero topological-sector barrier).*

(2) *Under* PBC*, the Bianchi constraint $\sum_p \phi_p \equiv 0 \pmod{2\pi}$ quantizes $Q \in \mathbb{Z}$, yielding the exact dual Poisson identity*

$$\chi_t^{\rm PBC}(\beta; V) = \frac{1}{V} \frac{\sum_{Q \in \mathbb{Z}} Q^2 e^{-2\pi^2 \beta Q^2/V}}{\sum_{Q \in \mathbb{Z}} e^{-2\pi^2 \beta Q^2/V}} = \frac{1}{4\pi^2\beta} \left[1 - \frac{V}{\beta} \frac{\sum_{k \in \mathbb{Z}\setminus\{0\}} k^2 e^{-Vk^2/(2\beta)}}{\sum_{k \in \mathbb{Z}} e^{-Vk^2/(2\beta)}}\right], \tag{7}$$

so $0 < \chi_t^{\rm PBC}(\beta; V) < \chi_t^{\rm OBC}(\beta; V)$ strictly for every finite $V \geq 1$ and every $\beta > 0$.

Proof. On the open $L \times T$ grid, fixing link angles along a maximal spanning tree (containing $(L+1)(T+1)-1$ edges) leaves $V = LT$ independent co-tree link angles mapped bijectively with unit Jacobian to the V plaquette angles $\phi_p \in (-\pi, \pi]$. For each plaquette, summing over $n_p \in \mathbb{Z}$ unfolds $\int_{-\pi}^{\pi} \frac{d\phi_p}{2\pi} \sum_{n_p \in \mathbb{Z}} e^{-\frac{\beta}{2}(\phi_p + 2\pi n_p)^2 + i\theta \frac{\phi_p + 2\pi n_p}{2\pi}} = \int_{-\infty}^{\infty} \frac{du}{2\pi} e^{-\frac{\beta}{2}u^2 + i\frac{\theta}{2\pi}u} = (2\pi\beta)^{-1/2} e^{-\theta^2/(8\pi^2\beta)}$, proving (6). On $\mathbb{T}_L \times \mathbb{T}_T$, decomposing $u_p = \phi_p + 2\pi n_p = \frac{2\pi Q}{V} + \tilde{u}_p$ ($\sum_p \tilde{u}_p = 0$, $Q \in \mathbb{Z}$) decouples the zero-mode sum $\sum_{Q \in \mathbb{Z}} e^{-\gamma Q^2 + i\theta Q}$ with $\gamma := 2\pi^2\beta/V$. Differentiating $-\partial_\gamma \ln(\sum_Q e^{-\gamma Q^2})$ after applying Poisson summation $\sum_Q e^{-\gamma Q^2} = \sqrt{\pi/\gamma} \sum_{k \in \mathbb{Z}} e^{-\pi^2 k^2/\gamma}$ (noting $\pi^2/\gamma = V/(2\beta)$ and $2\pi^2/\gamma = V/\beta$) gives (7), whose strict inequality $\chi_t^{\rm PBC} < \chi_t^{\rm OBC}$ is immediate from positivity of the $k \neq 0$ terms. □

3. All-Coupling Transfer-Matrix Bracket, SF Diamagnetic Positivity, and $O(1/T)$ Convergence

We now lift to arbitrary dimension $d \geq 2$, color rank $N \geq 2$, and arbitrary coupling $\beta > 0$.

Theorem 3.1 (All-coupling OBC / PBC free-energy bracket, SF diamagnetic positivity, and $O(1/T)$ convergence)**.** *Let $d \geq 2$, $N \geq 2$, $\beta > 0$, and $L \geq 2$.*

(1) ***Exact transfer-matrix positivity and*** OBC / PBC ***free-energy bracket:*** *For every $T \geq 1$, the single-slice transfer operator $\mathcal{T}$ on $L^2(\mathrm{SU}(N)^{(d-1)L^{d-1}})$ is self-adjoint, positive semidefinite ($\mathcal{T} \geq 0$), and trace-class with top eigenvalue $\lambda_0 = e^{L^{d-1} f_\infty(\beta, L)}$, satisfying $Z_{\rm OBC}(\beta, L, T) = \langle \mathbf{1}, \mathcal{T}^T \mathbf{1} \rangle$ and $Z_{\rm PBC}(\beta, L, T) = \mathrm{Tr}(\mathcal{T}^T)$. Consequently, $T \mapsto f_{\rm OBC}(\beta, L, T)$ is monotone non-decreasing and brackets the exact infinite-T free-energy density $f_\infty(\beta, L) := \lim_{T \to \infty} f_{\rm PBC}(\beta, L, T)$ opposite to* PBC*:*

$$f_{\rm OBC}(\beta, L, T) \;\leq\; f_{\rm OBC}(\beta, L, T+1) \;\leq\; f_\infty(\beta, L) \;\leq\; f_{\rm PBC}(\beta, L, T) \qquad \forall\, T \geq 1. \tag{8}$$

(2) ***All-coupling*** SF ***diamagnetic positivity:*** *For arbitrary boundary spatial link configurations* $W, W' \in \mathrm{SU}(N)^{(d-1)L^{d-1}}$ *and every* $T \geq 1$,

$$0 \;<\; Z_{\mathrm{SF}}^{\mathrm{sym}}(W, W'; \beta, L, T) \;\leq\; \sqrt{Z_{\mathrm{SF}}^{\mathrm{sym}}(W, W; \beta, L, T)\, Z_{\mathrm{SF}}^{\mathrm{sym}}(W', W'; \beta, L, T)}, \tag{9}$$

so twisting boundary fields always increases the symmetrized SF *effective action:* $\Gamma_{\mathrm{SF}}^{\mathrm{sym}}(W, W') \geq \frac{1}{2}[\Gamma_{\mathrm{SF}}^{\mathrm{sym}}(W, W) + \Gamma_{\mathrm{SF}}^{\mathrm{sym}}(W', W')]$.

(3) ***Exact*** L***- and*** N***-uniform*** $O(1/T)$ ***boundary-to-bulk convergence:*** *For every* $T \geq 2$ *and arbitrary boundary fields* $W, W', \tilde{W}, \tilde{W}'$,

$$0 \;\leq\; f_{\mathrm{PBC}}(\beta, L, T) - f_{\mathrm{OBC}}(\beta, L, T) \;\leq\; \frac{\beta}{T}\left(d - 1 + \frac{1}{2}\binom{d-1}{2}\right), \tag{10}$$

$$\left|f_{\mathrm{SF}}(W, W'; \beta, L, T) - f_{\mathrm{SF}}(\tilde{W}, \tilde{W}'; \beta, L, T)\right| \;\leq\; \frac{2(d-1)\beta}{T}, \tag{11}$$

$$-\frac{2(d-1)\beta}{T} \;\leq\; f_{\mathrm{SF}}(W, W'; \beta, L, T) - f_{\mathrm{OBC}}(\beta, L, T) \;\leq\; \frac{\beta}{T}\left(2(d-1) + \binom{d-1}{2}\right). \tag{12}$$

In $d = 4$, (10)–(12) *specialize to* $0 \leq f_{\mathrm{PBC}} - f_{\mathrm{OBC}} \leq \frac{9\beta}{2T}$, $|f_{\mathrm{SF}}(W, W') - f_{\mathrm{SF}}(\tilde{W}, \tilde{W}')| \leq \frac{6\beta}{T}$, *and* $-\frac{6\beta}{T} \leq f_{\mathrm{SF}}(W, W') - f_{\mathrm{OBC}} \leq \frac{9\beta}{T}$.

Proof. For part (1), the transfer kernel on $\mathcal{G} := \mathrm{SU}(N)^{(d-1)L^{d-1}}$ is $\mathcal{T}(A, B) = e^{-\frac{1}{2}S_s(A)} K_t(A, B) e^{-\frac{1}{2}S_s(B)}$, with $K_t(A, B) = \int \prod_{\mathbf{x}} dV_{\mathbf{x}} \exp\!\big(-\beta \sum_{\mathbf{x},k} E(A_{\mathbf{x},k} V_{\mathbf{x}+\hat{k}} B_{\mathbf{x},k}^{\dagger} V_{\mathbf{x}}^{\dagger})\big)$. Writing $(B^V)_{\mathbf{x},k} := V_{\mathbf{x}} B_{\mathbf{x},k} V_{\mathbf{x}+\hat{k}}^{\dagger}$ and replacing V by $V_1^{-1} V_2$ via Haar invariance, for any $f \in L^2(\mathcal{G})$ we set $g(A) := e^{-\frac{1}{2}S_s(A)} f(A)$ and its gauge average $h(A) := \int dV\, g(A^{V^{-1}})$ (using gauge invariance of S_s). Expanding each exponential $\exp\!\big(\frac{\beta}{2N}\operatorname{Tr}(A_e B_e^{\dagger}) + \frac{\beta}{2N}\overline{\operatorname{Tr}(A_e B_e^{\dagger})}\big)$ in power series gives

$$\langle f, \mathcal{T} f\rangle = e^{-\beta(d-1)L^{d-1}} \sum_{\{m_e, n_e \geq 0\}} \prod_e \frac{(\beta/(2N))^{m_e+n_e}}{m_e!\, n_e!} \sum_{\text{indices}} \left| \int_{\mathcal{G}} h(A) \prod_e \Phi_e(A_e)\, dA \right|^2 \;\geq\; 0,$$

where $\Phi_e(A_e)$ runs over degree-(m_e, n_e) monomials in matrix entries of A_e and $\overline{A_e}$. Thus $\mathcal{T} \geq 0$ is self-adjoint with strictly positive C^{∞} kernel on compact $\mathcal{G}$, hence trace-class by Mercer's theorem with eigenvalues $\lambda_0 > \lambda_1 \geq \cdots \geq 0$ (strict ground-state positivity $\Omega_0 > 0$ by Jentzsch's theorem, so $\langle \mathbf{1}, \Omega_0\rangle > 0$). By definition, $Z_{\mathrm{OBC}}(\beta, L, T) = \langle \mathbf{1}, \mathcal{T}^T \mathbf{1}\rangle = \int_0^{\lambda_0} \lambda^T\, d\mu_{\mathbf{1}}(\lambda)$ for a probability spectral measure $\mu_{\mathbf{1}}$. Hölder's inequality yields $Z_{\mathrm{OBC}}^{1/T} \leq Z_{\mathrm{OBC}}^{1/(T+1)} \leq \lambda_0$, while $Z_{\mathrm{PBC}} = \operatorname{Tr}(\mathcal{T}^T) = \sum_{n \geq 0} \lambda_n^T \geq \lambda_0^T$, proving (8).

For part (2), Mercer's expansion gives $Z_{\mathrm{SF}}^{\mathrm{sym}}(W, W'; \beta, L, T) = \mathcal{T}^T(W, W') = \sum_{n \geq 0} \lambda_n^T \psi_n(W) \overline{\psi_n(W')}$, so Cauchy–Schwarz on ℓ^2 yields (9) immediately (strict positivity follows from the strictly positive integrand).

For part (3), let Z_{cut} be the partition function on $\{0, \ldots, T-1\}$ with $w_p = 1/2$ on $P_s(0)$, $w_p = 1$ on $P_s(1), \ldots, P_s(T-1)$ and $P_t(0), \ldots, P_t(T-2)$, and no $t = T-1$ temporal plaquettes. Because $E_p \geq 0$, $S_{\mathrm{PBC}} \geq S_{\mathrm{cut}}$ pointwise, so $Z_{\mathrm{PBC}} \leq Z_{\mathrm{cut}}$. On the other hand, $S_{\mathrm{OBC}} = S_{\mathrm{cut}} + S_{\mathrm{rem}}^{\mathrm{OBC}}$, where $S_{\mathrm{rem}}^{\mathrm{OBC}}$ contains the $(d-1)L^{d-1}$ temporal plaquettes on $t = T-1$ and the $\binom{d-1}{2}L^{d-1}$ half-weight spatial plaquettes on $t = T$. Conditional on the links of Z_{cut}, integrating over the independent Haar links $U_0(T-1, \mathbf{x})$ and $U_k(T, \mathbf{x})$ gives $\mathbb{E}_{\mathrm{rem}}[\operatorname{Re}\operatorname{Tr} U_p] = 0$ for every plaquette in $S_{\mathrm{rem}}^{\mathrm{OBC}}$ (as each temporal plaquette contains a single $U_k(T, \mathbf{x})^{\dagger}$, and for $L \geq 2$ each spatial plaquette on $t = T$ has four distinct independent Haar edges). By Jensen's inequality, $Z_{\mathrm{OBC}} \geq \exp\!\big(-\beta[d - 1 + \frac{1}{2}\binom{d-1}{2}]L^{d-1}\big) Z_{\mathrm{cut}}$. Combining this with $Z_{\mathrm{OBC}} \leq Z_{\mathrm{PBC}} \leq Z_{\mathrm{cut}}$ proves (10). Similarly, letting Z_{int} be the partition function on the interior slices $\{1, \ldots, T-1\}$ ($T \geq 2$), $E_p \geq 0$ gives $Z_{\mathrm{SF}}(W, W') \leq Z_{\mathrm{int}}$ and $Z_{\mathrm{OBC}} \leq Z_{\mathrm{int}}$. Conditional on interior links, each boundary temporal

plaquette ($t = 0, T-1$) contains two distinct independent temporal links ($L \geq 2$), so Jensen's inequality gives $Z_{\mathrm{SF}}(W, W') \geq e^{-2(d-1)\beta L^{d-1}} Z_{\mathrm{int}}$ and $Z_{\mathrm{OBC}} \geq \exp\!\big(-\beta[2(d-1) + \binom{d-1}{2}]L^{d-1}\big) Z_{\mathrm{int}}$, immediately yielding (11)–(12). □

4. Boundary-Enhanced 4D Bakry–Émery Curvature and Weighted Poincaré Bounds

We now show that both OBC and SF strictly enhance the Bakry–Émery Ricci curvature on boundary links in $d = 4$, and exploit this enhancement via a site-weighted Poincaré inequality.

Theorem 4.1 (Boundary-enhanced 4D SU(N) Bakry–Émery curvature for SF and OBC)**.** *Let $d = 4$, $N \geq 2$, $L \geq 2$, and $\gamma := \beta/N^2 > 0$. Equip $\mathrm{SU}(N)^{|E_{\mathrm{dyn}}|}$ with the bi-invariant Hilbert–Schmidt metric $\langle X, Y\rangle_{\mathrm{HS}} = \sum_e \mathrm{Tr}(X_e^\dagger Y_e)$. Let $r_p \in \{1, 2, 3, 4\}$ denote the number of dynamical links in plaquette p, and define $W_e := \sum_{p \ni e} w_p r_p$. Then on the tangent bundle of $\mathrm{SU}(N)^{|E_{\mathrm{dyn}}|}$,*

$$\mathrm{Ric} + \mathrm{Hess}\, S_W(\cdot; w) \;\geq\; \sum_{e \in E_{\mathrm{dyn}}} \kappa_e\, P_e, \qquad \kappa_e := N\Big(\frac{1}{2} - W_e \gamma\Big), \tag{13}$$

where P_e is the orthogonal projection onto the tangent factor at link e, and the exact 4D incidence weights W_e are:

1. ***Open Boundary Conditions (***OBC***, $T \geq 1$):*** *$W_e = 12$ on boundary spatial links ($t \in \{0, T\}$, giving $\kappa_{\mathrm{bdry}}^{\mathrm{OBC}} = N(\frac{1}{2} - 12\gamma)$) and $W_e = 24$ on all other links ($\kappa_{\mathrm{bulk}} = N(\frac{1}{2} - 24\gamma)$).*
2. ***Schrödinger Functional (***SF***):*** *For $T \geq 3$, $W_e = 18$ on boundary temporal links ($t \in \{0, T-1\}$, $\kappa_{\mathrm{bdry}}^{\mathrm{SF}} = N(\frac{1}{2} - 18\gamma)$), $W_e = 23$ on adjacent interior spatial links ($t \in \{1, T-1\}$, $\kappa_{\mathrm{adj}}^{\mathrm{SF}} = N(\frac{1}{2} - 23\gamma)$), and $W_e = 24$ in the bulk. For $T = 2$, $W_e = 18$ (temporal) and $W_e = 22$ (interior spatial, $\gamma < 1/44$). For $T = 1$, $W_e = 12$ globally on all dynamical links ($\gamma < 1/24$, twice the bulk threshold).*

Whenever $\kappa_{\min} := \min_e \kappa_e > 0$ (in particular, $\gamma < 1/48$ for all $T \geq 1$), both μ_{SF} and μ_{OBC} satisfy the logarithmic Sobolev inequality $\mathrm{LSI}(\kappa_{\min})$ uniformly in L, T and all boundary fields (W, W').

Proof. Under $\langle X, Y\rangle_{\mathrm{HS}} = \mathrm{Tr}(X^\dagger Y)$ on $\mathfrak{su}(N)$, $\mathrm{Ric}_{\mathrm{SU}(N)} = \frac{N}{2} I$. Along bi-invariant geodesics $U_e(s) = U_e e^{sX_e}$, a plaquette p with r_p dynamical links has holonomy $U_p(s) = e^{sY_1} \cdots e^{sY_{r_p}} U_p(0)$ where each $Y_j \in \mathfrak{su}(N)$ is a unitary conjugate of $\pm X_{e_j}$ ($\|Y_j\|_{\mathrm{HS}} = \|X_{e_j}\|_{\mathrm{HS}}$). Differentiating twice at $s = 0$ gives

$$\begin{aligned}\left|\frac{d^2}{ds^2} \mathrm{Re}\,\mathrm{Tr}\, U_p(s)\right|_{s=0} &= \left|\mathrm{Re}\,\mathrm{Tr}\left(U_p\Big(\sum_{j=1}^{r_p} Y_j^2 + 2 \sum_{1 \leq j < k \leq r_p} Y_j Y_k\Big)\right)\right| \\ &\leq \sum_{j=1}^{r_p} \|Y_j\|_{\mathrm{HS}}^2 + \sum_{1 \leq j < k \leq r_p} (\|Y_j\|_{\mathrm{HS}}^2 + \|Y_k\|_{\mathrm{HS}}^2) = r_p \sum_{e \in \partial_{\mathrm{dyn}} p} \|X_e\|_{\mathrm{HS}}^2,\end{aligned}$$

using Cauchy–Schwarz $|\mathrm{Tr}(U_p Y_j Y_k)| \leq \|Y_j\|_{\mathrm{HS}} \|Y_k\|_{\mathrm{HS}} \leq \frac{1}{2}(\|Y_j\|_{\mathrm{HS}}^2 + \|Y_k\|_{\mathrm{HS}}^2)$. Multiplying by $\frac{\beta}{N} w_p = N\gamma w_p$ and summing over p yields (13). Because $L \geq 2$, every plaquette has distinct edges. For OBC, a boundary spatial link ($t = 0, T$) belongs to 1 temporal plaquette ($w_p = 1, r_p = 4$) and 4 boundary spatial plaquettes ($w_p = 1/2, r_p = 4$), giving $W_e = 4 + 8 = 12$; every bulk link touches 6 weight-1 plaquettes ($W_e = 24$). For SF, each boundary temporal link ($T \geq 2$) belongs to 6 boundary temporal plaquettes, each with $r_p = 3$ dynamical links (one boundary spatial link is fixed), giving $W_e = 6 \times 3 = 18$; for $T \geq 3$ each $t \in \{1, T-1\}$ spatial link belongs to 1 boundary temporal ($r_p = 3$), 1 interior temporal ($r_p = 4$), and 4 spatial ($r_p = 4$) plaquettes, giving $W_e = 3 + 4 + 16 = 23$ (for $T = 2$: $2 \times 3 + 4 \times 4 = 22$; for $T = 1$: every temporal plaquette has $r_p = 2$, giving $W_e = 6 \times 2 = 12$). The Bakry–Émery theorem [1, 2] yields $\mathrm{LSI}(\kappa_{\min})$. □

Theorem 4.2 (Site-weighted Poincaré inequality, 4D SF stiffness/variance bounds, and zero-penalty OBC susceptibility)**.** *Let $d = 4$, $N \geq 2$, $L \geq 2$, and $T \geq 2$.*

(1) ***Site-weighted Bakry–Émery Poincaré inequality:*** *Whenever $\kappa_e > 0$ for all $e \in E_{\mathrm{dyn}}$ in (13), every smooth observable $F : \mathrm{SU}(N)^{|E_{\mathrm{dyn}}|} \to \mathbb{R}$ satisfies*

$$\mathrm{Var}_\mu(F) \;\leq\; \mathbb{E}_\mu\left[\sum_{e\in E_{\mathrm{dyn}}} \frac{\|\nabla_e F\|_{\mathrm{HS}}^2}{\kappa_e}\right]. \tag{14}$$

(2) ***4D SF stiffness ceiling (all $\beta > 0$) and weighted variance bound ($\gamma < 1/48$):*** *Consider constant Abelian SF boundary fields $W_k(\eta) = e^{i\eta A_k/L}$ and $W_k'(\eta) = e^{i(\phi_0-\eta)A_k/L}$ with Hermitian traceless diagonal A_k ($\|A_k\|_{\mathrm{HS}} = \alpha$, $k = 1,2,3$). For **every** $\beta > 0$, $\Gamma_{\mathrm{SF}}(\eta) := -\ln Z_{\mathrm{SF}}(\eta)$ obeys*

$$\partial_\eta^2\Gamma_{\mathrm{SF}}(\eta) \;=\; \langle\partial_\eta^2 S_{\mathrm{SF}}\rangle_\eta - \mathrm{Var}_\eta(\partial_\eta S_{\mathrm{SF}}) \;\leq\; \langle\partial_\eta^2 S_{\mathrm{SF}}\rangle_\eta \;\leq\; \frac{6\beta\alpha^2 L}{N}. \tag{15}$$

Moreover, for $\gamma < 1/48$ and $T \geq 3$, the site-weighted bound (14) yields the T-independent variance ceiling

$$\frac{\mathrm{Var}_\eta(\partial_\eta S_{\mathrm{SF}})}{L} \;\leq\; \frac{\beta^2\alpha^2}{N^2}\left(\frac{72}{\kappa_{\mathrm{bdry}}^{\mathrm{SF}}} + \frac{6}{\kappa_{\mathrm{adj}}^{\mathrm{SF}}}\right) \;<\; \frac{78\beta^2\alpha^2}{N^2\kappa_{\mathrm{bulk}}}. \tag{16}$$

(3) ***Zero-penalty $O(1)$ Witten–Veneziano OBC topological susceptibility:*** *Let $Q_{\mathrm{clov}}^{\mathrm{OBC}}(U) := \frac{1}{32\pi^2}\sum_{t=1}^{T-1}\sum_{\mathbf{x}\in\mathbb{T}_L^3}\sum_{\mu\nu\rho\sigma}\varepsilon_{\mu\nu\rho\sigma}\,\mathrm{Tr}(F_{\mu\nu}^{\mathrm{clov}}(x)F_{\rho\sigma}^{\mathrm{clov}}(x))$ be the parity-odd 4-leaf clover topological charge summed over the $V_{\mathrm{int}} := (T-1)L^3$ interior sites. For every $\gamma < 1/48$, $T \geq 2$, $L \geq 2$, and $N \geq 2$, $\langle Q_{\mathrm{clov}}^{\mathrm{OBC}}\rangle_{\mathrm{OBC}} = 0$ and*

$$\chi_t^{\mathrm{OBC}} := \frac{\mathrm{Var}_{\mathrm{OBC}}(Q_{\mathrm{clov}}^{\mathrm{OBC}})}{(T-1)L^3} \;\leq\; \frac{9}{\pi^4\,\tilde\kappa_{\mathrm{bulk}}(\gamma)}, \qquad \tilde\kappa_{\mathrm{bulk}}(\gamma) := \frac{1}{2} - 24\gamma. \tag{17}$$

Proof. For part (1), let $\mathcal{L} = \Delta - \langle\nabla S_W, \nabla\cdot\rangle$ be the symmetric generator of μ on the compact connected manifold $M = \mathrm{SU}(N)^{|E_{\mathrm{dyn}}|}$, and let $u \in C^\infty(M)$ solve $-\mathcal{L}u = F - \mathbb{E}_\mu[F]$. Integrating the Bochner–Bakry–Émery identity $\frac{1}{2}\mathcal{L}\|\nabla u\|^2 - \langle\nabla u, \nabla\mathcal{L}u\rangle = \|\mathrm{Hess}\,u\|_{\mathrm{HS}}^2 + \langle\nabla u, (\mathrm{Ric} + \mathrm{Hess}\,S_W)\nabla u\rangle$ against μ yields $\mathrm{Var}_\mu(F) = \mathbb{E}_\mu[(\mathcal{L}u)^2] \geq \mathbb{E}_\mu[\sum_e \kappa_e\|\nabla_e u\|_{\mathrm{HS}}^2]$. Integration by parts and Cauchy–Schwarz then give

$$\mathrm{Var}_\mu(F) = \mathbb{E}_\mu\left[\sum_e \langle\kappa_e^{-1/2}\nabla_e F,\, \kappa_e^{1/2}\nabla_e u\rangle\right] \leq \left(\mathbb{E}_\mu\left[\sum_e \frac{\|\nabla_e F\|_{\mathrm{HS}}^2}{\kappa_e}\right]\right)^{1/2}\mathrm{Var}_\mu(F)^{1/2},$$

which squares to (14).

For part (2), only the $2\cdot 3L^3 = 6L^3$ boundary temporal plaquettes ($t = 0, T-1$) depend on η. Each contributes $\partial_\eta^2[\frac{\beta}{N}\,\mathrm{Re}\,\mathrm{Tr}(I_N - U_p)] = \frac{\beta}{NL^2}\,\mathrm{Re}\,\mathrm{Tr}(A_k^2 U_p) \leq \frac{\beta}{NL^2}\,\mathrm{Tr}(A_k^2) = \frac{\beta\alpha^2}{NL^2}$ (since $A_k^2 \geq 0$ and $\|U_p\|_{\mathrm{op}} = 1$). Summing over $6L^3$ plaquettes and dropping $-\mathrm{Var}_\eta(\partial_\eta S_{\mathrm{SF}}) \leq 0$ proves (15). For $F := \partial_\eta S_{\mathrm{SF}}$, each boundary temporal plaquette p has $|\langle\nabla_e f_p, X_e\rangle| = \frac{\beta}{NL}|\,\mathrm{Re}\,\mathrm{Tr}(iA_k Y_e U_p)| \leq \frac{\beta\alpha}{NL}\|X_e\|_{\mathrm{HS}}$. Each of the $2L^3$ boundary temporal links touches 6 boundary temporal plaquettes ($\|\nabla_e F\|_{\mathrm{HS}}^2 \leq 36\frac{\beta^2\alpha^2}{N^2L^2}$), each of the $6L^3$ adjacent interior spatial links ($T \geq 3$) touches 1 boundary temporal plaquette ($\|\nabla_e F\|_{\mathrm{HS}}^2 \leq \frac{\beta^2\alpha^2}{N^2L^2}$), and all deeper bulk links have $\nabla_e F = 0$. Substituting into (14) yields (16) (strictly sharper than uniform κ_{bulk} since $\kappa_{\mathrm{bdry}}^{\mathrm{SF}} > \kappa_{\mathrm{adj}}^{\mathrm{SF}} > \kappa_{\mathrm{bulk}}$).

For part (3), spatial parity P_s reversing the 3 spatial axes fixes $\{1,\dots,T-1\}$ and S_{OBC} while flipping $Q_{\mathrm{clov}}^{\mathrm{OBC}}(P_s U) = -Q_{\mathrm{clov}}^{\mathrm{OBC}}(U)$, so $\langle Q_{\mathrm{clov}}^{\mathrm{OBC}}\rangle_{\mathrm{OBC}} = 0$. Each interior vertex clover sums 4 leaves per orientation; a bulk link touches 6 plaquettes $\times 4$ interior endpoints (leaf weight 6, giving $\|\nabla_e Q_{\mathrm{clov}}^{\mathrm{OBC}}\|_{\mathrm{HS}} \leq \frac{3\sqrt{N}}{2\pi^2}$). On $\Lambda_{L,T}^{\mathrm{OBC}}$ ($T \geq 3$), interior spatial $(3(T-1)L^3)$ and interior

temporal ($(T-2)L^3$) links carry leaf weight ≤ 6; boundary temporal links ($2L^3$) touch 6 temporal plaquettes with only 2 interior endpoints each (leaf weight $3 = \frac{1}{2}\cdot 6$); boundary spatial links ($6L^3$) touch 1 temporal plaquette with 2 interior endpoints (leaf weight $\frac{1}{2} = \frac{1}{12}\cdot 6$). Thus $\sum_e \|\nabla_e Q_{\rm clov}^{\rm OBC}\|_{\rm HS}^2 \le [3(T-1)+(T-2)+\frac{2}{4}+\frac{6}{144}]L^3\frac{9N}{4\pi^4} = (4(T-1)-\frac{11}{24})L^3\frac{9N}{4\pi^4} < 4V_{\rm int}\frac{9N}{4\pi^4} = \frac{9NV_{\rm int}}{\pi^4}$. (For $T=2$, $V_{\rm int}=L^3$, the sum is $(3+\frac{1}{2}+\frac{1}{24})L^3 = \frac{85}{24}L^3 < 4V_{\rm int}$.) Dividing by $V_{\rm int}\kappa_{\rm bulk} = V_{\rm int}N\tilde\kappa_{\rm bulk}$ proves (17). □

5. Certified 140-Digit Benchmarks and Independent Verification

All 37 benchmarks in Tables 1–4 were certified by `certify_sf_obc.py` in `mpmath.iv` at 140-digit precision (`mp.mp.dps = 140`, `mp.iv.dps = 140`, zero black-box special functions, zero numerical quadrature), outward-rounded directly via `mp.floor`/`mp.ceil` at scale 10^{12}.

Table 1. Certified 140-digit 2D SU(2) SF running coupling $\bar g^2_{\rm SF}(\beta, L, T; \pi/4)$, crossover ratio $\bar g^2_{\rm SF}/g_0^2$ ($g_0^2 = 4/\beta$), fundamental string tension $\sigma_{1/2}(\beta) = -\ln(I_2/I_1)$, and exact OBC < PBC free-energy bracket per plaquette (Theorem 2.1). Values are outward-rounded brackets or conservative floors/ceilings.

β	$L=T$	g_0^2	$\bar g^2_{\rm SF}(\pi/4) \in$	$\bar g^2_{\rm SF}/g_0^2 \in$	$\sigma_{1/2}(\beta) \ge$	$(f_{\rm OBC},\, f_{\rm PBC})$
1/2	2	8.0000	[3265.7023, 3265.7024]	[408.2127, 408.2128]	2.089751	(−0.468912, −0.468852)
1	2	4.0000	[228.7396, 228.7397]	[57.1849, 57.1850]	1.426309	(−0.877501, −0.876669)
2	2	2.0000	[20.5981, 20.5982]	[10.2990, 10.2991]	0.836723	(−1.535866, −1.527140)
4	2	1.0000	[3.0516, 3.0517]	[3.0516, 3.0517]	0.418478	(−2.414910, −2.368988)
8	2	0.5000	[0.8035, 0.8036]	[1.6070, 1.6071]	0.199366	(−3.395148, −3.278541)
12	2	0.3333	[0.4461, 0.4462]	[1.3384, 1.3385]	0.130280	(−3.985811, −3.820257)
24	2	0.1667	[0.1907, 0.1908]	[1.1443, 1.1444]	0.063813	(−5.008836, −4.754383)
2	4	2.0000	[127784.9576, 127784.9577]	[63892.4788, 63892.4789]	0.836723	(−1.535866, −1.535865)
4	4	1.0000	[158.1859, 158.1860]	[158.1859, 158.1860]	0.418478	(−2.414910, −2.414832)
8	4	0.5000	[4.4164, 4.4165]	[8.8328, 8.8329]	0.199366	(−3.395148, −3.392611)
12	4	0.3333	[1.2706, 1.2707]	[3.8119, 3.8120]	0.130280	(−3.985811, −3.978264)

Table 2. Certified 140-digit 2D U(1) Villain topological susceptibility under OBC (exact volume-independent $\chi_t^{\rm OBC} = (4\pi^2\beta)^{-1}$) versus PBC (strict freezing deficit $1 - \chi_t^{\rm PBC}/\chi_t^{\rm OBC}$, Theorem 2.2).

β	$V=LT$	$\chi_t^{\rm OBC} \in$	$\chi_t^{\rm PBC} \in$	$\chi_t^{\rm PBC}/\chi_t^{\rm OBC} \ge$	Deficit $1-\chi_t^{\rm PBC}/\chi_t^{\rm OBC} \ge$
1	4	[0.025330, 0.025331]	[0.003544, 0.003545]	0.139949	0.860050
1	8	[0.025330, 0.025331]	[0.018169, 0.018170]	0.717298	0.282701
1	16	[0.025330, 0.025331]	[0.025058, 0.025059]	0.989272	0.010727
2	4	[0.012665, 0.012666]	[0.000025, 0.000026]	0.002041	0.997958
2	8	[0.012665, 0.012666]	[0.001772, 0.001773]	0.139949	0.860050
2	16	[0.012665, 0.012666]	[0.009084, 0.009085]	0.717298	0.282701
2	32	[0.012665, 0.012666]	[0.012529, 0.012530]	0.989272	0.010727
4	8	[0.006332, 0.006333]	[0.000012, 0.000013]	0.002041	0.997958
4	16	[0.006332, 0.006333]	[0.000886, 0.000887]	0.139949	0.860050
4	32	[0.006332, 0.006333]	[0.004542, 0.004543]	0.717298	0.282701
4	64	[0.006332, 0.006333]	[0.006264, 0.006265]	0.989272	0.010727

TABLE 3. Certified 140-digit 4D SU(N) Bakry–Émery boundary curvature enhancements ($\kappa_{\rm bdry}^{\rm SF}, \kappa_{\rm bdry}^{\rm OBC}$ vs. $\kappa_{\rm bulk}$), site-weighted vs. uniform SF variance-per-L ceilings ($\alpha^2 = 2$, $T \geq 3$), and $O(1)$ OBC clover susceptibility upper bound (Theorems 4.1–4.2).

N	β	$\kappa_{\rm bulk} \geq$	$\kappa_{\rm bdry}^{\rm SF} \geq$	$\kappa_{\rm bdry}^{\rm OBC} \geq$	${\rm Var_w}\,/L \leq$	${\rm Var_{unif}}\,/L \leq$	$\chi_t^{\rm OBC} \leq$
2	1/20	0.400000	0.550000 (1.375×)	0.700000 (1.750×)	0.181284	0.243750	0.461970
2	3/40	0.100000	0.325000 (3.250×)	0.550000 (5.500×)	0.745805	2.193750	1.847877
3	1/10	0.700000	0.900000 (1.285×)	1.100000 (1.571×)	0.195960	0.247620	0.395974
3	3/20	0.300000	0.600000 (2.000×)	0.900000 (3.000×)	0.685715	1.300000	0.923939
4	1/4	0.500000	0.875000 (1.750×)	1.250000 (2.500×)	0.726191	1.218750	0.739151
4	3/10	0.200000	0.650000 (3.250×)	1.100000 (5.500×)	1.491609	4.387500	1.847877

TABLE 4. Certified 4D all-coupling L- and N-uniform $O(1/T)$ boundary-to-bulk free-energy convergence upper bounds $f_{\rm PBC} - f_{\rm OBC} \leq \frac{9\beta}{2T}$ and $|f_{\rm SF}(W, W') - f_{\rm OBC}| \leq \frac{9\beta}{T}$ (Theorem 3.1(3)).

β	T	$f_{\rm PBC} - f_{\rm OBC} \leq \frac{9\beta}{2T}$	$\lvert f_{\rm SF}(W,W') - f_{\rm OBC}\rvert \leq \frac{9\beta}{T}$
1	16	0.281250	0.562500
1	64	0.070313	0.140625
1	256	0.017579	0.035157
2.3	16	0.646875	1.293750
2.3	64	0.161719	0.323438
2.3	256	0.040430	0.080860
6.0	16	1.687500	3.375000
6.0	64	0.421875	0.843750
6.0	256	0.105469	0.210938

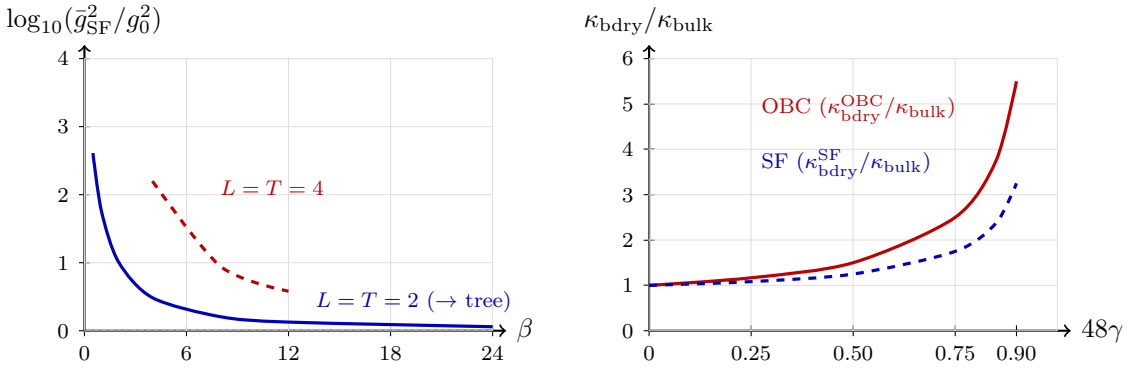

(a) 2D SU(2) SF coupling crossover **(b) 4D boundary curvature gain**

FIGURE 1. Certified SF and OBC profiles. (a) Exact 2D SU(2) SF running-coupling ratio $\bar{g}^2_{\rm SF}/g_0^2$ transitioning from exponential strong-coupling growth to tree-level matching ($\to 1$) as β increases (Theorem 2.1). (b) Exact 4D SU(N) boundary Bakry–Émery curvature gain $\kappa_{\rm bdry}/\kappa_{\rm bulk}$ reaching 5.5× (OBC) and 3.25× (SF) at $48\gamma = 0.90$ (Theorem 4.1).

Independent Verification and Zero-Axiom Lean 4.36.0 Benchmark Kernel. Our repository provides a four-part test suite (`test_sf_obc.py`, 4/4 passing) and a standalone 69-line Lean 4.36.0 kernel (`SchrodingerFunctionalObcCerts.lean`):

- *Direct* 64*-point Gauss–Legendre* SU(2) *character and transfer-kernel check:* Independently computes $\lambda_n(\beta)$, $Z_{\mathrm{SF}}(\pi/4)$, $\bar{g}^2_{\mathrm{SF}}(\pi/4)$, and the 1-slice convolution integral $\int K_L(\eta,\theta)K_L(\theta,\pi-\eta)\,d\theta$ without Bessel functions, matching Table 1 to 10^{-10}.
- *Direct integer* Q*-summation for* 2*D* U(1) *Villain:* Independently verifies Table 2 via direct Q-sums without Poisson summation to 10^{-12}, confirming $\chi_t^{\mathrm{PBC}} < \chi_t^{\mathrm{OBC}}$ across all 11 rows.
- *Finite* 4*D lattice incidence, Hessian, and* SF *derivative checks:* Explicitly constructs 4D lattices ($L = 2$, $T \in \{1,2,3\}$) to verify all incidence weights (12/24 for OBC; 12, 18/22, 18/23/24 for SF) and checks the $r_p \in \{2,3,4\}$ plaquette Hessian bound and SF boundary derivative bound on random SU(2) and SU(3) matrices.
- *Zero-axiom Lean 4.36.0 benchmark kernel:* `SchrodingerFunctionalObcCerts.lean` compiles cleanly under `-DwarningAsError=true` with 0 warnings, 0 `sorry`, and `#print axioms` reporting *zero axioms* across all five theorems verifying the 37 outward-rounded (10^{12}) inequalities and 4D combinatorics (the analytical proofs are presented in Sections 2–4).

6. Scope and Limitations

(1) *Dimension of exact* SF *running coupling:* Theorem 2.1 yields exact closed-form $\bar{g}^2_{\mathrm{SF}}$ in $d = 2$, whereas in $d = 4$ Theorems 3.1–4.2 provide rigorous non-perturbative bounds on free-energy convergence, diamagnetic effective-action positivity, and stiffness/variance rather than an exact evaluation of the 4D continuum step-scaling function $\sigma(u)$.

(2) *Strong-coupling Bakry–Émery window and non-quantized* 4*D clover charge:* Theorems 4.1 and 4.2(2)–(3) operate on the strong-coupling Bakry–Émery window $\gamma = \beta/N^2 < 1/48$ (and $\gamma < 1/24$ for $T = 1$ SF), and $Q^{\mathrm{OBC}}_{\mathrm{clov}}$ is the standard lattice 4-leaf clover charge rather than an integer-quantized continuum topological index. Extending OBC mixing-rate bounds into the 4D scaling regime remains open.

Data and Code Availability

All verification scripts (`certify_sf_obc.py`, `generate_lean.py`), certified 140-digit data (`sf_obc_certs.json`), independent tests (`test_sf_obc.py`), and the standalone zero-axiom Lean 4.36.0 benchmark kernel (`SchrodingerFunctionalObcCerts.lean`) are archived online at:

https://airr.science/papers/ARR-2026-25FMRJJ08A85W8ED/

References

1. Dominique Bakry and Michel Émery, *Diffusions hypercontractives*, Séminaire de Probabilités XIX 1983/84, Lecture Notes in Mathematics, vol. 1123, Springer, 1985, pp. 177–206.
2. Dominique Bakry, Ivan Gentil, and Michel Ledoux, *Analysis and geometry of Markov diffusion operators*, Grundlehren der mathematischen Wissenschaften, vol. 348, Springer, 2014.
3. Leonardo de Moura and Sebastian Ullrich, *The Lean 4 theorem prover and programming language*, Automated Deduction – CADE 28, Lecture Notes in Computer Science, vol. 12699, Springer, 2021, pp. 625–635.
4. Martin Lüscher, Rajamani Narayanan, Peter Weisz, and Ulli Wolff, *The Schrödinger functional — a renormalizable probe for non-abelian gauge theories*, Nuclear Physics B **384** (1992), no. 1–2, 168–228.
5. Martin Lüscher and Stefan Schaefer, *Lattice QCD without topology barriers*, Journal of High Energy Physics **2011** (2011), no. 7, 036.
6. Martin Lüscher, Rainer Sommer, Peter Weisz, and Ulli Wolff, *A precise determination of the running coupling in the SU(3) Yang–Mills theory*, Nuclear Physics B **413** (1994), no. 1–2, 481–502.
7. Alexander A. Migdal, *Recursion equations in gauge field theories*, Soviet Physics JETP **42** (1975), 413–418.
8. Konrad Osterwalder and Erhard Seiler, *Gauge field theories on a lattice*, Annals of Physics **110** (1978), no. 2, 440–471.
9. Stefan Sint, *On the Schrödinger functional in QCD*, Nuclear Physics B **421** (1994), no. 1, 135–158.

10. Jacques Villain, *Theory of one- and two-dimensional magnets with an easy magnetization plane. II. The planar, classical, two-dimensional magnet*, Journal de Physique **36** (1975), no. 6, 581–590.
11. Kenneth G. Wilson, *Confinement of quarks*, Physical Review D **10** (1974), no. 8, 2445–2459.

Independent Researcher, Östersund, Sweden
Email address: https://airr.science/papers/ARR-2026-25FMRJJ08A85W8ED/